Processing of natural time series of intensities by the visual system of the blowfly

Hateren, J.H. van

Published in:
Vision Research

Publication date:
1997

Pergamon

PII: S0042-6989(97)00105-3

Vision Res., Vol. 37, No. 23, pp. 3407–3416, 1997

Printed in Great Britain
0042-6989/97 $17.00 + 0.00

Processing of Natural Time Series of Intensities by the Visual System of the Blowfly

J. H. VAN HATEREN*

Received 16 July 1996; in revised form 8 January 1997

A major problem that a visual system faces is how to fit the large intensity variation of natural image streams into the limited dynamic range of its neurons. One of the means to accomplish this is through the use of gain control. In order to investigate this, natural time series of intensities were measured, as well as the responses of blowfly photoreceptors and Large Monopolar Cells (LMCs) to these time series. Time series representative of what each photoreceptor of a real visual system would normally receive were measured with an optical system measuring the light intensity of a spot comparable with the field of view of single human foveal cones. This system was worn on a headband by a freely walking person. Resulting time series have rms-contrasts ranging from an average of 0.45 for 1-sec segments to 1.39 for 100-sec segments (both when limited to frequencies up to 100 Hz). Power spectra behave approximately as $1/f$ (f: temporal frequency). Measured time series were subsequently presented to fly photoreceptors and LMCs by playing them back on an LED. The results show that fast gain controls indeed keep the response within the dynamic range of the cells and that a large part of this range is actually used for packing the information in natural time series. © 1997 Elsevier Science Ltd

Natural light intensities Temporal power spectrum Photoreceptor LMC Gain control

INTRODUCTION

Images entering an eye change continuously in time, not only because objects in the outside world may move, but also because eyes are moving themselves. A major problem a visual system faces is how to fit the large variance of these natural image streams into the limited dynamic range of its neurons (Laughlin, 1981; Srinivasan *et al.*, 1982). Recent theories of early visual processing attempt to solve this problem with the help of information theory (e.g. Atick & Redlich, 1990; Bialek *et al.*, 1991; van Hateren, 1992a; Linsker, 1993; Nadal & Parga, 1994) or reconstruction criteria (Ruderman, 1994b). The results are theoretical filters that are designed to either reduce redundancy, maximize information, or maximize fidelity. All theories utilize the characteristic second-order statistics of natural images, i.e., the $1/f_s^2$-behaviour of their power spectra (e.g. Field, 1987; van der Schaaf & van Hateren, 1996), and subject the system to some constraint, like keeping a minimum amount of information (Atick & Redlich, 1990) or keeping the response within the response range of the neuron (van Hateren, 1992a). Predicted filters generally agree well with measurements of contrast sensitivities or impulse responses (Atick & Redlich, 1990; Atick, 1992; van Hateren, 1992a, 1993; Dong & Atick, 1995a). For more natural stimuli, theoretical predictions have been compared with measurements in the fly visual system (van Hateren, 1992c) and in cat LGN neurons (Dan *et al.*, 1996); again, there is a satisfactory correspondence between theory and experiment. Nevertheless, detailed examination of the case of the fly (van Hateren, 1992c) suggests that the real neural system is more sophisticated than the theory. The main difference is that at a given background light level, the theoretical filters are fixed and linear, whereas the neurons adapt to local properties of the stimulus, such as the local average of light intensity. Part of this adaptation is very fast, with a significant change in gain within a few tens of milliseconds. Furthermore, for the theoretical optimizations gaussian statistics are assumed, whereas the real visual input is non-gaussian (Laughlin, 1981; Richards, 1982; Ruderman & Bialek, 1994). Processing strategies that handle these non-gaussian, usually very skewed, statistics were discussed by, for example, Laughlin (1981, 1983), Ruderman & Bialek (1994), and Ruderman (1994a). Nevertheless, as a result of skewed stimulus statistics, the theoretical models of spatiotemporal preprocessing at present do not handle the large variability of light intensities and contrasts found in any particular outdoor scene as well as real visual systems do.

In order to gain some insight into how the early visual system handles natural scenes through adaptation, time series of natural intensities were measured, as well as the responses of fly photoreceptors and second-order neurons

*Department of Biophysics, University of Groningen, Nijenborgh 4, NL-9747 AG Groningen, The Netherlands *Fax*: + 31.50.3634740; *Email*: hateren@bcn.rug.nl.

(the Large Monopolar Cells, or LMCs) to these time series. The reason for using time series as a stimulus rather than full spatiotemporal stimuli is two-fold. First, time series of intensities can both be measured and reproduced in the laboratory faithfully, with virtually the same dynamic range as they occur in natural environments. This is not attainable for full spatiotemporal data, at least not with reasonable means: in particular display equipment can not yet reach the high luminances, high contrasts and high speeds required to reproduce natural stimulus statistics accurately. Second, the analysis of responses to time series is simpler, and sufficiently complete as far as fly photoreceptors are concerned (fly photoreceptors are not spatially coupled). The long-term goal of this approach is to use the experimental data as a benchmark for the development and evaluation of quantitative models of (light) adaptation that can be related to the statistics of the natural environment, and that thus have a functional interpretation.

METHODS

Measurement of natural time series

As the goal of this study is to investigate responses of photoreceptors and LMCs to natural time series of intensities, it is important to obtain time series that are representative of the ones normally encountered by a photoreceptor. This depends not only on the properties of the visual environment, but also on the behaviour of the visual system: how fast does it move, by what trajectory does it scan the surroundings, will it spend more time looking at particular parts of the scene than at others (e.g., avoiding looking at the sky for a long time), and so on. Ideally, these data should be obtained for the animal under study, behaving naturally in its natural habitat. For the fly, this is difficult to obtain with sufficient accuracy. Therefore, we decided to obtain time series for the human visual system instead (van Hateren & van der Schaaf, 1996), and use those for analysis and for stimuli to the fly visual system. The temporal structure of these data is expected to be roughly equivalent to those normally encountered by the fly (see Discussion). We constructed a small optical device, consisting of a lens (Photar 1:4/50), colour filters (Schott BG38 and KG3), a diaphragm of approximately 40 μm in front of a light guide, and a photomultiplier (Hamamatsu H5783-01) at the other end of the light guide. Intensity data from the photomultiplier were digitally recorded on a portable DAT-recorder (Sony PC-208A). The resulting detector has a spectral sensitivity not very different from the photopic sensitivity of the human eye, an angular resolution of a few arcminutes, i.e., of the same order of magnitude as that of human foveal and parafoveal vision, a temporal resolution better than 1 kHz, and the total system is linear in intensity over more than four orders of magnitude.

The optical system was mounted on a headband, worn by a freely walking person. Although this device follows the direction of gaze of the head, movements of the eyes relative to the head are not accounted for; in fact, this would be technically difficult to achieve with cone accuracy in a fully portable system. As a simpler approach, the subject wore marked glasses, and was instructed to minimize eye movements (by keeping the markers at a fixed position in the visual field) by substituting head movements for eye movements. In addition, measurements were performed by holding the detector in hand during walking, and pointing it in varying directions; this gave similar results as the head-based measurements. Obviously, these measurements must be considered as only a crude approximation of what would result when real eye dynamics are taken into account. Yet, the obtained time series of light intensities are most likely close enough to those actually encountered by photoreceptors to enable a meaningful analysis of light adaptation in natural circumstances.

Stimuli and electrophysiology

Measured time series were presented to the visual system of the blowfly (*Calliphora vicina*) by playing them back, at a rate of 1200 samples/sec, on a superbright LED (Toshiba TLGD109P, spectral peak at 567 nm), producing light intensities comparable with daylight conditions. At maximum brightness, the LED produced a steady photoreceptor depolarization of approximately 28 mV, corresponding to almost 10^7 photons/sec (van Hateren, 1992a). An LED with its collimating lens intact was used as a wide-field stimulus (field diameter approximately 15 deg) for photoreceptors or LMCs. An LED with the lens removed was used as a narrow-field stimulus (1.5 deg diameter), which is approximately equivalent to a point source for LMCs (their receptive field has a full width at half-height of 1–1.5 deg). Both wide-field and narrow-field stimuli had approximately the same effective intensity, yielding similar depolarizations in the photoreceptors. The responses of photoreceptors and LMCs (graded changes of their membrane potential) were measured using an intracellular glass micropipette (for details see van Hateren, 1992a). Responses were amplified and digitized at a rate of 1200 samples/sec for further analysis. Each of the results presented below is supported by stable recordings in at least three different cells. Unless stated otherwise, data were low-pass filtered to 100 Hz (by block averaging) in order to reduce noise.

RESULTS

Figure 1 shows a typical example of a 1-sec trace of intensity measurements [Fig. 1(A)], and the resulting responses in a fly photoreceptor cell [Fig. 1(B)], an LMC with narrow-field illumination [Fig. 1(C)], and an LMC with wide-field illumination [Fig. 1(D)]. The trace of [Fig. 1(A)] shows the typical properties of natural time series of intensities: many sharp and large peaks rising from a relatively low baseline, with occasional large steps in intensity. The response of the photoreceptor more or less follows the incoming light intensity, although with several modifications. Both large peaks and large steps in average intensity are reduced in amplitude. Smaller

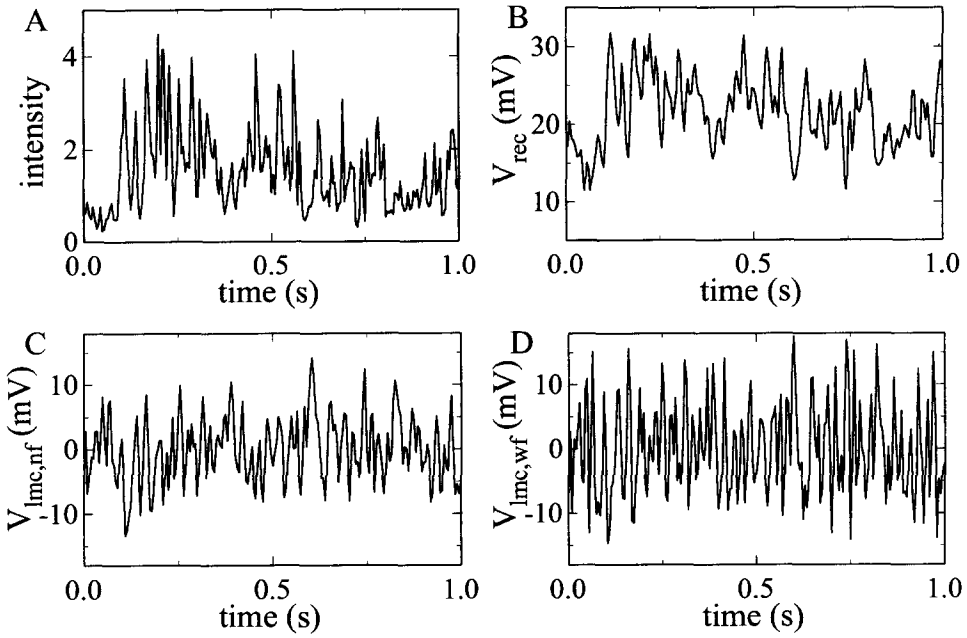

FIGURE 1. Time traces of natural intensities and the resulting responses in fly photoreceptors and LMCs, all limited to 100 Hz. (A) Intensity (in arbitrary units). (B) Response of a photoreceptor cell to the intensity series shown in (A). (C) Response of an LMC to the intensity series of (A), presented as a narrow-field stimulus. (D) Response of an LMC to the intensity series of (A), presented as a wide-field stimulus. The responses in (B), (C), and (D) are given relative to the resting potentials of the cells. Fly photoreceptors depolarize in response to light, whereas the LMCs hyperpolarize in response to an increment in light intensity.

signal variations are well preserved. The behaviour is roughly equivalent to that of a logarithmic transformation, although it appears to be different when examined closely. Whereas a logarithmic transform is a static nonlinearity, acting immediately, the photoreceptor has a more dynamic behaviour. The mechanism it uses is a constant adjustment of its gain, where the adjustment has both very fast and relatively slow components.

The response of the LMC, [Fig. 1(C)] and [Fig. 1(D)], is very different from that of the photoreceptor. First of all the sign of the response is reversed: whereas photoreceptors depolarize in response to an increment in intensity, LMCs hyperpolarize. In addition to that, fully light-adapted LMCs more or less differentiate the photoreceptor signal, which can be seen in Fig. 1 as the LMC response leading the intensity and photoreceptor traces (positive intensity steps yield negative LMC peaks). Finally, Fig. 1 shows that the characteristics of the signal gradually change when going from intensity through photoreceptor to LMC: whereas the signal in Fig. 1(A) has many low intensity values with fewer high intensity peaks, the finally resulting wide-field LMC response in Fig. 1(D) is much more evenly distributed over its response range.

The average power spectrum of consecutive sections of the time series is shown in Fig. 2 (a: intensity; b: photoreceptor response; c: LMC response to narrow-field illumination; and d: LMC response to wide-field illumination). The fact that the power spectrum in Fig. 2(a) follows approximately a straight line on a log–log scale shows that it behaves as $1/f_t^{\gamma}$, with f_t the temporal frequency, and γ here close to 1 (compare the lower dashed line, which has a slope of -1). For frequencies higher than approximately 100 Hz (not shown), the power spectrum starts to deviate from a straight line because the signal is low-pass filtered by the spatial aperture of the light detector, in combination with the upper limit of (angular) velocities produced by the subject carrying the detector. As can be seen in Fig. 2, the power spectrum of the receptor potential (trace b) also

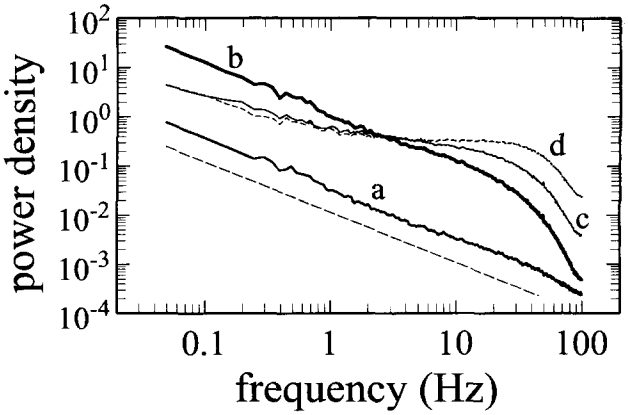

FIGURE 2. Power spectra of a 45 minute stretch of intensity data (a), and the resulting responses in a photoreceptor (b), in an LMC with narrow-field illumination (c), and in an LMC with wide-field illumination (d). The power spectra were obtained by averaging the power spectra of consecutive sections (of 20.48 sec) of each measurement. The lower dashed line shows the slope of a $1/f_t$ power spectrum. Power density is normalized to the average intensity for (a), thus giving $(\text{contrast})^2\text{Hz}^{-1}$; for (b), (c), and (d) the units are $(\text{mV})^2\text{Hz}^{-1}$.

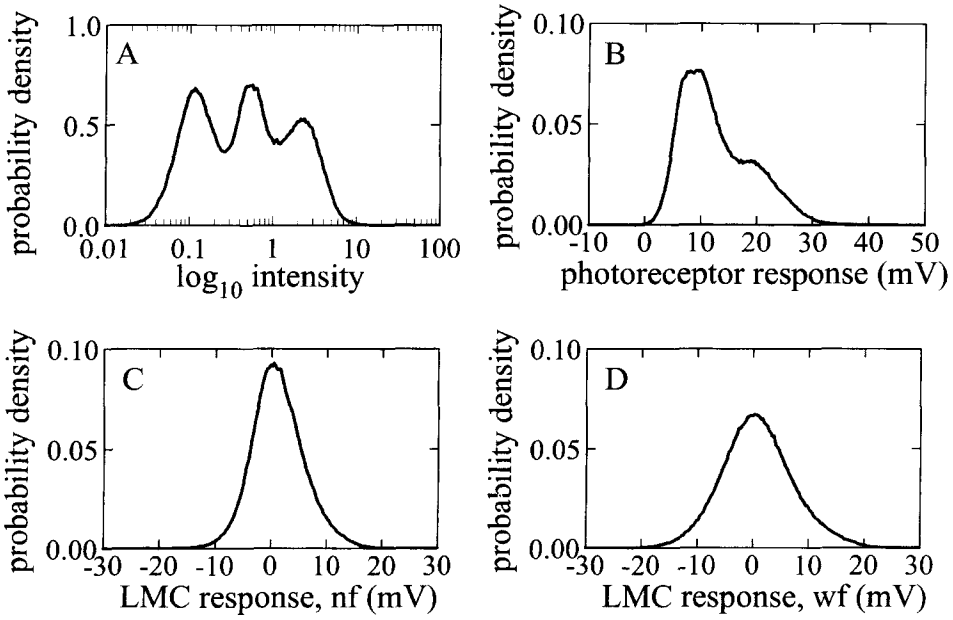

FIGURE 3. Probability density of a stretch of 45 min of intensity measurements (A) and the resulting responses in a photoreceptor (B), in an LMC with narrow-field illumination (C), and in an LMC with wide-field illumination (D). The units of the probability densities are $[\log_{10}(\text{intensity})]^{-1}$ in (A), and $(\text{mV})^{-1}$ in (B), (C), and (D).

goes as $1/f_t$, up to frequencies where the temporal low-pass filtering by the photoreceptor becomes dominant. The power spectra for the LMC (traces c and d) do not follow the $1/f_t$ behaviour: these spectra become almost flat over a substantial range of frequencies, in particular for wide-field illumination [Fig. 2(d)].

Figure 3 shows probability densities for the intensity and resulting photoreceptor and LMC responses, calculated for a 45 min stretch of continuous measurements taken during a walk outside (on a sunny day, in an environment of meadows and wood). The histogram in Fig. 3(A) was collected after taking the logarithm of the measured light intensities. As can be seen, the distribution of light intensities is quite broad, with most values falling in a range of 2.5–3 log units (the range is 2.3 log units for less than 10^{-2} outliers, i.e., 5×10^{-3} at the low intensity end and 5×10^{-3} at the high intensity end of the distribution, and the range is 2.9 for $<10^{-4}$ outliers). Note that the roughly symmetrical distribution on a log scale implies a very skewed distribution on a linear scale: most intensities are at the low end of the (linear) distribution, with a long tail of high intensity peaks (see e.g., Laughlin, 1981; Richards, 1982). Figure 3(B) shows the probability density of the photoreceptor response (on a linear scale) to the same 45 min stretch of intensities. The range is 28 mV for $<10^{-2}$ outliers, and 40 mV for $<10^{-4}$. Thus, a large part of the available response range of the photoreceptor cell (approximately 60 mV) is actually used when responding to this natural series of intensities. The same applies to the responses of LMCs as shown in Fig. 3(C) and (D) (narrow-field and wide-field stimulation). For $<10^{-2}$ outliers, the response ranges are 26 and 33 mV, and for $<10^{-4}$ outliers 41 and 45 mV, respectively. Furthermore, the distribution becomes very symmetrical.

The skewed distribution of intensity values, as in Fig. 3(A), can produce values higher than 1 for the rms-contrast, defined as the ratio of the standard deviation and the mean in a particular time segment. This is only the case for relatively long time segments, though, as the rms-contrast depends on the segment length. For data limited to 100 Hz, the rms-contrast was 0.25 ± 0.05 for 0.1 sec segments, 0.45 ± 0.10 for 1 sec, 0.81 ± 0.25 for 10 sec, 1.39 ± 0.55 for 100 sec, and 1.86 ± 0.65 for 45 min (averages and standard deviations for consecutive segments in 17 measurements of 45 min, performed by six different subjects under various weather conditions and in various environments). Laughlin (1981, 1983) reports an average contrast of 0.4 for spatial scans over a range of 25–50 deg, using a light detector with a spatial aperture comparable with that of a fly photoreceptor. This is consistent with the values above if we assume a scanning speed of approximately 50 deg/sec, which is of the right order of magnitude for flying flies.

How much do the distributions as shown in Fig. 3 vary over time? To analyse this question, the 45 min measurements were divided into shorter segments, of which histograms were made. Figure 4 shows a few representative examples of a total of 45, 1-min segments thus analysed. As can be seen, the intensity histograms vary considerably in shape and width, even on a log-scale, and the photoreceptor histograms vary only slightly less (but now on a linear scale). The LMC histograms, on the other hand, are remarkably constant. This is further analysed in Fig. 5. For two time scales (1-min segments: open circles, and 5-sec segments: dots) the relation between various response measures is compared. Figure

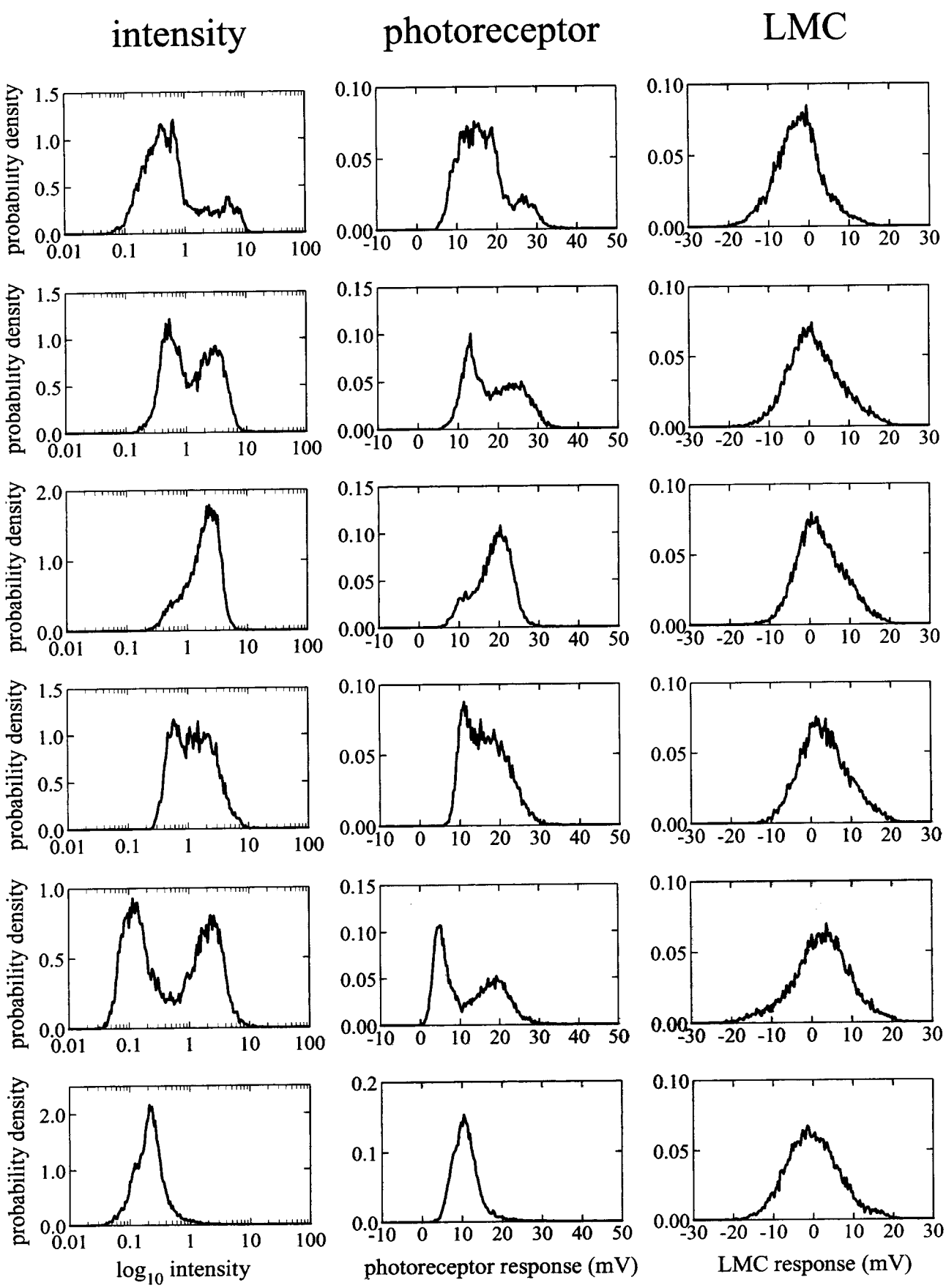

FIGURE 4. Probability densities as in Fig. 3(A), (B), and (D), here for several 1-min segments taken from a total of 45 min (consecutive rows are for minutes 1, 5, 9, 15, 18, and 23). Units as in Fig. 3.

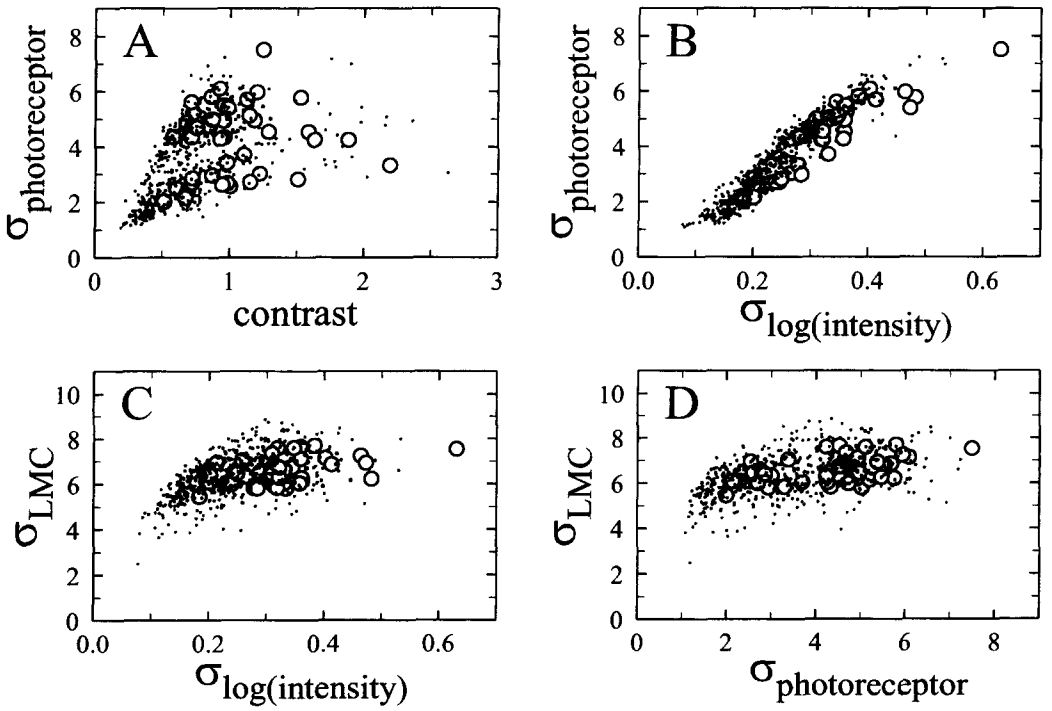

FIGURE 5. Relation between various measures of variability for time series of intensity, and the resulting response of a photoreceptor and an LMC with wide-field illumination. Data points are either for 45 consecutive 1-min segments (open circles), or for 540 consecutive 5-sec segments (dots), taken from the same 45-min data set. Contrast is defined as the standard deviation of the light intensity in a particular segment divided by the average intensity in that segment; for 1-min segments the average contrast was 1.00 ± 0.36 (SD), for 5-sec segments 0.73 ± 0.35; $\sigma_{\log(\text{intensity})}$ is the standard deviation of the decimal logarithm of the intensities in a segment, $\sigma_{\text{photoreceptor}}$ the standard deviation (in mV) of the photoreceptor response in a segment, and σ_{LMC} (also in mV) that of the LMC response in a segment. Correlation coefficients for the 1-min and 5-sec data are: 0.12 and 0.53 (A), 0.91 and 0.95 (B), 0.49 and 0.52 (C), 0.51 and 0.47 (D). See text for further explanation.

5(A) shows how the intensity contrast (calculated per segment as the ratio of the standard deviation and the mean) is related to the standard deviation of the photoreceptor response. These measures correlate, but not very strongly. As shown in Fig. 5(B), a much stronger correlation is obtained when using the standard deviation of the logarithmically transformed intensity rather than contrast. Figure 5(C) compares this contrast measure with the LMC response distribution. As suggested already by Fig. 4, the LMC fills its response range almost independently of the input contrast [see also Fig. 5(D), with photoreceptor and LMC standard deviations compared]. This is not only the case for 1-min segments (open circles) but also for 5-sec segments (dots). Only for rather small input contrasts, does the response distribution become significantly smaller. These results suggest that LMCs are, in effect, executing a form of contrast normalization in the time domain.

DISCUSSION

The main results presented here are that the very skewed intensity distributions of natural time series become more compact when first transduced by the photoreceptor and then further processed by the LMC. As a result, natural stimuli efficiently utilize a large part of the available response range of both cell types. Furthermore, it was shown that power spectra of both light intensity and receptor potential show a $1/f_t$-behaviour, whereas the LMC, in particular when illuminated with a wide field stimulus, makes the power spectrum almost flat. Finally, the LMC appears to fill its response range almost independently of the local contrast in natural time series, thus, in effect, showing a form of contrast normalization.

Although the intensity measurements were obtained with the help of a human subject carrying the detector, the resulting time series are probably not very different from those that would have resulted if similar measurements could have been done with the fly. The reason is as follows. Let us suppose that a photoreceptor with an acceptance angle $\Delta\rho$ scans, with an angular speed ω, a textured object or a cluster of objects at a distance d. Then the resulting time series of intensities could also have been obtained, at least approximately, by using a photoreceptor with an acceptance angle $2\Delta\rho$, scanning, with an angular speed 2ω, an object at a distance $d/2$. The smaller distance is compensated by both the larger acceptance angle (to get the spatial resolution right) and the higher scanning speed (to get the temporal succession of intensities right). When comparing the fly and the human visual systems, these three factors seem to scale approximately as required: the acceptance angle is much larger for flies than for humans (approximately 1 deg and

1′, respectively); the average angular speed is much higher (where the order of magnitude may be 100 deg/sec for flies and 1 deg/sec for humans; for a discussion see van Hateren, 1992a, 1993); and the average distance to the closest objects is much smaller in flies than in humans. There are no quantitative data available on the latter factor, but the order of magnitude appears to be at least approximately right for the above scaling to work. Of course, the real situation is much more complicated because of the 3-D structure of both the environment and the locomotion of the organism, but to a first-order approximation we may expect that the time series for humans and flies are roughly similar. The temporal cut-off frequency of the time series (i.e., the point where the power spectrum drops below the $1/f_t$-line) is proportional to average angular speed, and inversely proportional to the acceptance angle of the photoreceptors, and will thus be approximately the same for both flies and humans.

Figure 3(B) shows that the response distributions in the photoreceptor and the LMC are relatively well behaved: much of the response range is used with a reasonable frequency of occurrence, which means that the available information capacity is better utilized than the original intensity distribution [Fig. 3(A) on a linear scale] would have produced (in other words, much of the first-order redundancy has been removed). Arguments along similar lines have been presented previously (Laughlin, 1981; Richards, 1982; Ruderman & Bialek, 1994). Response distributions of fly photoreceptors and LMCs have been measured before, but only for non-natural stimuli such as white noise of moderate contrast (e.g., Juusola *et al.*, 1995; de Ruyter van Steveninck & Laughlin, 1996). These responses occupy a much smaller range than reported here for natural stimuli.

Figure 2 (trace b), on the other hand, shows that there is still much second-order redundancy present in the photoreceptor signal (it is still correlated in time). Much of this second-order redundancy is, in fact, removed during transmission from photoreceptors to second-order neurons (as shown by the almost flat trace d in Fig. 2). This is consistent with recent theories of early visual processing based on information theoretic arguments (redundancy reduction: Atick & Redlich, 1990, 1992; information maximization: Linsker, 1993, see also Linsker, 1988; a similar theory based on information maximization was independently developed by van Hateren, 1992a,b, 1993). These theories predict whitening of the spatiotemporal input, at least at high signal-to-noise ratios. This whitening was recently shown directly for LGN neurons in cats viewing video sequences (Dan *et al.*, 1996).

Power spectra of time series

It has been shown by several investigators (e.g. Burton & Moorhead, 1987; Field, 1987, 1993; Tolhurst *et al.*, 1992; Ruderman & Bialek, 1994; van der Schaaf & van Hateren, 1996) that the power spectra of images behave as approximately $1/f_s^2$, with f_s spatial frequency. A time series can be considered as a scan over a spatial image, and we may thus expect a relation between spatial and temporal power spectra. Indeed, assuming random phases in the spatial spectrum and a fixed velocity of scanning, the temporal power spectrum resulting from $1/f_s^{\alpha}$ should run as $1/f_t^{\alpha-1}$ (this follows from considering a scan line as the product of a line mask and the image, which is equivalent to a convolution in the frequency domain with a perpendicular line, i.e., with integrating out one of the spatial frequency axes; random phases imply this integration should be performed on the power spectrum). Thus, the $1/f_t$-behaviour of the temporal power spectrum we found is consistent with a $1/f_s^2$-behaviour of the spatial power spectrum of images. In reality, the situation is more complicated. During translation of the visual system the visual scene changes as well. Characteristic time constants in the scanning behaviour by the visual system may complicate things further. In fact, for frequencies lower than 0.1–1 Hz, the power spectra deviate somewhat from a strict power-law behaviour, resulting in a less steep power spectrum for very low temporal frequencies (van der Schaaf and van Hateren, unpublished).

The $1/f_t$-behaviour of the temporal power spectrum should also be consistent with the full spatiotemporal power spectrum, as measured by Dong & Atick (1995b). They modelled these spectra, derived from video sequences, as $F(f_t/f_s)/f_s^{\alpha+1}$, with F a function of velocity and α the coefficient of the spatial power spectrum (i.e., $\alpha \approx 2$). A model of the same form was conjectured by van Hateren (1992a). The $1/f_t$-behaviour should follow from integrating the spatiotemporal power spectrum over all spatial frequencies (if we assume a very narrow acceptance angle of the light detector). Indeed, it is possible to derive that both $1/f_s^{\alpha}$ and $1/f_t^{\alpha-1}$ are consistent with the above spatiotemporal power spectrum (Ruderman, Dong, personal communications).

Is early vision linear or nonlinear?

Early vision is commonly viewed and modelled as a basically linear transformation (e.g. DeValois & De Valois, 1988; Atick & Redlich, 1990; van Hateren, 1992a). As information processing must involve essential nonlinearities at some stage at least, this view implies that early vision has more to do with data conditioning (such as bringing the sensory data into a representation that is suitable for further transport or processing) than with information processing in the sense of selecting and discarding information. It appears, though, that the data shown in Figs 3 and 5 are difficult to reconcile with this view of early vision as a linear process. Firstly, the photoreceptor transforms intensity in a highly nonlinear manner. Secondly, the subsequent contrast normalization by the LMC is a further nonlinear process. Of course, when using low contrast stimuli, linearity is still a reasonable assumption. However, the point is, that natural time series (and consequently natural image series as well) appear to keep both photoreceptor and LMC out of their linear range most of the time. Linearity is then more a laboratory condition than a realistic

operating mode of the visual system in natural circumstances. Consequently, theories of early vision must include nonlinearities and adaptation mechanisms if they are to produce computational schemes that adequately describe natural vision. Furthermore, this point stresses the value of using natural stimuli, or stimuli with selected natural statistics, because it makes it less likely to miss adaptational mechanisms that appear to be absent with statistically less rich stimuli, but that are in fact strongly active during normal vision.

The nonlinearity of early vision in the fly was investigated earlier by Laughlin (1981); (for generalizations of this scheme see Nadal & Parga, 1994; and Bell & Sejnowski, 1995). Laughlin showed that the static stimulus–response nonlinearity in LMCs approximately fits the requirements of histogram equalization: the nonlinearity reshapes the very skewed distribution of input contrasts into a flat response distribution. A flat distribution is optimal for an information channel with its response constrained by fixed limits (Shannon, 1948). If, on the other hand, the information channel is constrained by a fixed response variance (equivalent to power dissipation in an electrical transmission line), the optimal output distribution is a gaussian (Shannon, 1948). The LMC response is probably subject to a mixture of both constraints: the reversal potentials of the ions involved place a hard limit on the response range, but at the same time more power may be dissipated when the membrane potential is driven, in either direction, far from its resting level, owing to increased ion currents. The LMC physiology is not yet known in sufficient detail to quantify these factors. However, the LMC response distribution for the present stimulus is clearly closer to a gaussian than to a flat distribution. But it remains to be seen if this is also the case for full spatiotemporal natural stimuli of the same dynamics, luminance, and contrast as those encountered during natural locomotion of the fly.

Laughlin's scheme for response equalization could be modified such that the output distribution becomes more gaussian. Another modification that it would need is adaptation to local stimulus statistics: as Figs 4 and 5 show, the contrast normalization works for different contrast distributions of the input. Thus, a fixed stimulus–response nonlinearity, as in Laughlin (1981), is not sufficient. Interestingly, Ruderman & Bialek (1994) and Ruderman (1994a) recently presented a theory that adapts to local stimulus statistics by contrast normalization in such a way that it produces gaussian output distributions. When applied to static images, the algorithm consists of first taking the logarithm of the image intensities, and then dividing by a local estimate of the image contrast. This is a nonlinear procedure, and in fact Ruderman and Bialek could not find any linear filter that produces gaussian distributions. Applying the algorithm of Ruderman and Bialek to the time series measured here did, unfortunately, not produce gaussian distributions. One difference with the spatial case that may explain this failure is that high contrasts in images are often produced by edges, protruding into the surround used for the contrast estimate. The surround thus gives information about the contrast at its centre. For time series of intensities, on the other hand, an edge usually hits the photodetector without warning. For full spatiotemporal stimuli a warning about an upcoming moving edge may be transmitted from parts of the visual system that are spatially upstream, but this information is not available in the purely temporal stimulus used here. Still, the LMC performs very well, and it thus remains to be seen how the processing schemes of Laughlin and of Ruderman and Bialek can be reconciled with the processing in the fly visual system.

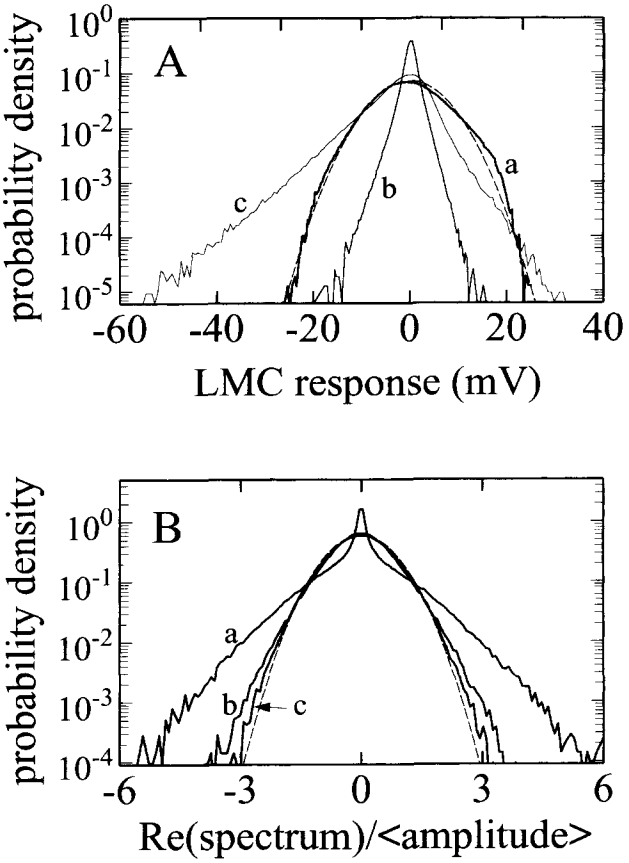

FIGURE 6. (A) a: the probability density of the response of an LMC with wide-field illumination [also shown in Fig. 3(D)], with a gaussian (dashed line) for comparison; b: probability density of the temporal derivative of the photoreceptor signal; c: probability density of the photoreceptor signal filtered with a minimum phase filter with the power transfer required by the photoreceptor and LMC power spectra of Fig. 2. (B) Probability density of the real part of the amplitude spectrum relative to the average value at each frequency; a: intensity; b: photoreceptor response; c: LMC response to wide-field stimulation. The dashed line shows a gaussian for comparison.

Gaussian or non-gaussian statistics?

As mentioned above, the shape of the probability density of the various parameters has theoretical implications, and will therefore be investigated in more detail here. As shown in Fig. 3, the LMC probability density (D) appears roughly gaussian. In Fig. 6(A), trace a, Fig. 3(D) is redrawn, but now with a logarithmic

abscissa. The dashed line is a parabola, which shows that the LMC probability density is indeed close to a gaussian. As the LMC approximately differentiates the photoreceptor response (actually performing a high-pass filtering which flattens the $1/f_t$ stimulus power spectrum, which is equivalent to multiplication of the amplitude spectrum by $f_t^{0.5}$, i.e., a fractional differentiation), it may be hypothesized that the probability density of Fig. 3(D) just results from differentiating the photoreceptor response. The result of that operation [Fig. 6(A), trace b] is in fact very different from the one actually measured in LMCs (trace a). In a slightly more sophisticated attempt to produce the LMC probability density by linear filtering, a high-pass filter was constructed with a power transfer just right to transform the photoreceptor power spectrum (Fig. 2, trace b) into that of the LMC (Fig. 2, trace d). The phase of the filter was constructed by assuming a minimum phase system (apart from a pure time delay this is a reasonable assumption for fly LMCs, see van Hateren, 1992a). Although this filter produced the correct power spectrum, the resulting probability density [Fig. 6(A), trace c] is again very different from the one measured in LMCs. The most direct approach for estimating the filtering by the LMC synapse, calculating the amplitude and phase of its transfer function from those of the measured responses in photoreceptors and LMCs, failed. It did not produce fixed, temporally localized impulse responses (calculated while carefully taking care of measurement noise), and thus it gave a temporal response in LMCs totally different from the measured one. The most likely explanation for this failure is that the assumption, linear transfer, is incorrect. These results further support the claim that the photoreceptor–LMC transformation must indeed be nonlinear in order to explain the data. A similar argument about the necessity for nonlinearities was given by Ruderman & Bialek (1994). As with spatial data, it is probably the very long correlation distances in the temporal data that prevent an easy, linear gaussification of the stimulus.

Another important issue is the probability density of each frequency component of the spectra. Many of the theories developed in recent years for deriving optimized filters for early visual processing implicitly assume gaussian statistics, in particular when applying Shannon's equation (Shannon, 1948) for obtaining information rates from signal to noise ratios (Atick & Redlich, 1990; van Hateren, 1992a; Ruderman, 1994b). Given the non-gaussian nature of natural images, this introduces uncertainty with regard to the question to what extent the predicted filters remain optimal when the actual statistics deviate from the idealized gaussian case (Ruderman, 1994b; but see Nadal & Parga, 1994). In order to investigate this, the following analysis was performed. If the power spectra were those of gaussian white noise, the probability density of the real or imaginary parts of the corresponding Fourier spectra should be gaussian (see e.g. Goldman, 1953). As the spectra are here not flat, but colored by $1/f_t$, the probability densities are expected to scale accordingly with frequency. Taking this into account, Fig. 6(B) shows the probability density for the real component of the spectra (a: intensity; b: photoreceptor; c: LMC wide-field illumination), at each frequency normalized by the average amplitude of the spectra at that frequency, and averaged over frequency. Thus, it shows the relative variation of the real component. The probability density is independent of frequency (as expected from white noise), and the results for the imaginary component are similar (both not shown). The parabola (dashed line) shows that, although the intensity power spectrum is highly non-gaussian, the power spectra of photoreceptors and, in particular, of LMCs are close to what would be expected if the spectra had been those of gaussian noise. Thus, it appears that a significant part of the non-gaussian nature of the temporal properties of natural images is removed by the first steps of visual processing. This suggests that the filters predicted by the abovementioned theories can be expected to be reasonably close to optimality when applied to intensities as transformed by the photoreceptors, even if this may not be the case when applied directly to the stimulus intensities themselves.

REFERENCES

Atick, J. J. (1992). Could information theory provide an ecological theory of sensory processing? *Network, 3*, 213–251.

Atick, J. J. & Redlich, A. N. (1990). Towards a theory of early visual processing. *Neural Computation, 2*, 308–320.

Bell, A. J. & Sejnowski, T. J. (1995). An information maximization approach to blind separation and blind deconvolution. *Neural Computation, 7*, 1129–1159.

Bialek, W., Ruderman, D. L. & Zee, A. (1991). Optimal sampling of natural images: a design principle for the visual system? In Lippmann, R. P., Moody, J. E. & Touretzky, D. S. (Eds), *Neural information processing systems 3* (pp. 363–369). San Mateo: Morgan Kaufmann.

Burton, G. J. & Moorhead, I. R. (1987). Color and spatial structure in natural scenes. *Applied Optics, 26*, 157–170.

Dan, Y., Atick, J. J. & Reid, R. C. (1996). Efficient coding of natural scenes in the lateral geniculate nucleus: experimental test of a computational theory. *Journal of Neuroscience, 16*, 3351–3362.

DeValois, R. L. & DeValois, K. K. (1988). *Spatial vision*. New York: Oxford University Press.

Dong, D. W. & Atick, J. J. (1995a) Temporal decorrelation: a theory of lagged and nonlagged responses in the lateral geniculate nucleus. *Network: Computation in Neural Systems, 6*, 159–178.

Dong, D. W. & Atick, J. J. (1995b) Statistics of natural time-varying images. *Network: Computation in Neural Systems, 6*, 345–358.

Field, D.J. (1987). Relations between the statistics of natural images and the response properties of cortical cells. *Journal of the Optical Society of America A, 4*, 2379–2394.

Field, D. J. (1993). Scale-invariance and self-similar "wavelet" transforms: an analysis of natural scenes and mammalian visual systems. In Farge, M., Hunt, J. C. R. & Vassilicos, J. C. (Eds), *Wavelets, fractals, and Fourier transforms* (pp. 151–193). Oxford: Clarendon Press.

Goldman, S. (1953). *Information theory*. New York: Dover Publications.

van Hateren, J. H. (1992a) Theoretical predictions of spatiotemporal receptive fields of fly LMCs, and experimental validation. *Journal of Comparative Physiology A, 171*, 157–170.

van Hateren, J. H. (1992b) A theory of maximizing sensory information. *Biological Cybernetics, 68*, 23–29.

van Hateren, J. H. (1992c) Real and optimal neural images in early vision. *Nature, 360*, 68–70.

van Hateren, J. H. (1993). Spatiotemporal contrast sensitivity of early vision. *Vision Research, 33*, 257–267.

van Hateren, J. H. & van der Schaaf, A. (1996). Temporal properties of natural scenes. In *Proceedings of the IS&T/SPIE Conference on Electronic Imaging: Science and Technology* (Vol. 2657, pp. 139–143). San Jose: SPIE.

Juusola, M., Uusitalo, R. O. & Weckström, M. (1995). Transfer of graded potentials at the photoreceptor–interneuron synapse. *Journal of General Physiology, 105*, 117–148.

Laughlin, S. B. (1981). A simple coding procedure enhances a neuron's information capacity. *Zeitschrift fur Naturforschung, 36c*, 910–912.

Laughlin, S. B. (1983). Matching coding to scenes to enhance efficiency. In Braddick, O. J. & Sleigh, A. C. (Eds), Physical and biological processing of images (pp. 42–52). New York: Springer.

Linsker, R. (1988). Self-organization in a perceptual network. Computer, March 1988, pp. 105-117.

Linsker, R. (1993). Deriving receptive fields using an optimal encoding criterion. In Hanson, S. J., Cowan, J. & Giles, C. L. (Eds), *Advances in neural information processing systems 5* (pp. 953–960). San Mateo: Morgan Kaufmann.

Nadal, J.-P. & Parga, N. (1994). Nonlinear neurons in the low-noise limit: a factorial code maximizes information transfer. *Network, 5*, 565–581.

Richards, W. A. (1982). Lightness scale from image intensity distributions. *Applied Optics, 21*, 2569–2582.

Ruderman, D. L. (1994a) The statistics of natural images. *Network: Computation in Neural Systems, 5*, 517–548.

Ruderman, D. L. (1994b) Designing receptive fields for highest fidelity. *Network: Computation in Neural Systems, 5*, 147–155.

Ruderman, D. L. & Bialek, W. (1994). Statistics of natural images: scaling in the woods. *Physics Review Letters, 73*, 814–817.

de Ruyter van Steveninck, R.R. & Laughlin, S.B. (1996). The rate of information transfer at graded potential synapses. *Nature, 379*, 642–645.

van der Schaaf, A. & van Hateren, J. H. (1996). Modelling the power spectra of natural images: statistics and information. *Vision Research, 36*, 2759–2770.

Shannon, C. E. (1948). The mathematical theory of communication. *Bell System Technical Journal, 27*, 3–91.

Srinivasan, M. V., Laughlin, S. B. & Dubs, A. (1982). Predictive coding: a fresh view of inhibition in the retina. *Proceedings of the Royal Society London B, 216*, 427–459.

Tolhurst, D. J., Tadmor, Y. & Chao, T. (1992). Amplitude spectra of natural images. *Ophthalmology and Physiological Optics, 12*, 229–232..

Acknowledgements—I thank Simon Laughlin, Arjen van der Schaaf, Herman Snippe, and Doekele Stavenga for comments on the manuscript. This research was supported by the Netherlands Organization for Scientific Research.